CLEO CONF 97-25
EPS97 365

Study of 3-prong hadronic τ decays with charged kaons

CLEO Collaboration

(August 15, 1997)

Abstract

Using a sample of 4.4 fb^{-1} integrated luminosity accumulated with the CLEO-II detector at the Cornell Electron Storage Ring (CESR), we have measured the ratios of branching fractions $Br(\tau^- \to K^-h^+\pi^-\nu_\tau)/Br(\tau^- \to h^-h^+h^-\nu_\tau) = (4.98 \pm 0.23 \pm 0.69) \times 10^{-2}$, $Br(\tau^- \to K^-h^+\pi^-\pi^0\nu_\tau)/Br(\tau^- \to h^-h^+h^-\pi^0\nu_\tau) = (2.64 \pm 0.47 \pm 0.48) \times 10^{-2}$, $Br(\tau^- \to K^-K^+\pi^-\nu_\tau)/Br(\tau^- \to h^-h^+h^-\nu_\tau) = (1.63 \pm 0.17 \pm 0.27) \times 10^{-2}$, and $Br(\tau^- \to K^-K^+\pi^-\pi^0\nu_\tau)/Br(\tau^- \to h^-h^+h^-\pi^0\nu_\tau) = (0.75 \pm 0.41 \pm 0.15) \times 10^{-2}$, corresponding to a 95% C.L. upper limit: $Br(\tau^- \to K^-K^+\pi^-\pi^0\nu_\tau)/Br(\tau^- \to h^-h^+h^-\pi^0\nu_\tau) <0.0148$.

B. Nemati,[1] S. J. Richichi,[1] W. R. Ross,[1] P. Skubic,[1] M. Bishai,[2] J. Fast,[2] J. W. Hinson,[2] N. Menon,[2] D. H. Miller,[2] E. I. Shibata,[2] I. P. J. Shipsey,[2] M. Yurko,[2] S. Glenn,[3] S. D. Johnson,[3] Y. Kwon,[3,*] S. Roberts,[3] E. H. Thorndike,[3] C. P. Jessop,[4] K. Lingel,[4] H. Marsiske,[4] M. L. Perl,[4] D. Ugolini,[4] R. Wang,[4] X. Zhou,[4] T. E. Coan,[5] V. Fadeyev,[5] I. Korolkov,[5] Y. Maravin,[5] I. Narsky,[5] V. Shelkov,[5] J. Staeck,[5] R. Stroynowski,[5] I. Volobouev,[5] J. Ye,[5] M. Artuso,[6] A. Efimov,[6] M. Goldberg,[6] D. He,[6] S. Kopp,[6] G. C. Moneti,[6] R. Mountain,[6] S. Schuh,[6] T. Skwarnicki,[6] S. Stone,[6] G. Viehhauser,[6] X. Xing,[6] J. Bartelt,[7] S. E. Csorna,[7] V. Jain,[7,†] K. W. McLean,[7] S. Marka,[7] R. Godang,[8] K. Kinoshita,[8] I. C. Lai,[8] P. Pomianowski,[8] S. Schrenk,[8] G. Bonvicini,[9] D. Cinabro,[9] R. Greene,[9] L. P. Perera,[9] G. J. Zhou,[9] B. Barish,[10] M. Chadha,[10] S. Chan,[10] G. Eigen,[10] J. S. Miller,[10] C. O'Grady,[10] M. Schmidtler,[10] J. Urheim,[10] A. J. Weinstein,[10] F. Würthwein,[10] D. W. Bliss,[11] G. Masek,[11] H. P. Paar,[11] S. Prell,[11] M. Sivertz,[11] V. Sharma,[11] D. M. Asner,[12] J. Gronberg,[12] T. S. Hill,[12] D. J. Lange,[12] S. Menary,[12] R. J. Morrison,[12] H. N. Nelson,[12] T. K. Nelson,[12] C. Qiao,[12] J. D. Richman,[12] D. Roberts,[12] A. Ryd,[12] M. S. Witherell,[12] R. Balest,[13] B. H. Behrens,[13] W. T. Ford,[13] H. Park,[13] J. Roy,[13] J. G. Smith,[13] J. P. Alexander,[14] C. Bebek,[14] B. E. Berger,[14] K. Berkelman,[14] K. Bloom,[14] D. G. Cassel,[14] H. A. Cho,[14] D. S. Crowcroft,[14] M. Dickson,[14] P. S. Drell,[14] K. M. Ecklund,[14] R. Ehrlich,[14] A. D. Foland,[14] P. Gaidarev,[14] R. S. Galik,[14] L. Gibbons,[14] B. Gittelman,[14] S. W. Gray,[14] D. L. Hartill,[14] B. K. Heltsley,[14] P. I. Hopman,[14] J. Kandaswamy,[14] P. C. Kim,[14] D. L. Kreinick,[14] T. Lee,[14] Y. Liu,[14] G. S. Ludwig,[14] N. B. Mistry,[14] C. R. Ng,[14] E. Nordberg,[14] M. Ogg,[14,‡] J. R. Patterson,[14] D. Peterson,[14] D. Riley,[14] A. Soffer,[14] B. Valant-Spaight,[14] C. Ward,[14] M. Athanas,[15] P. Avery,[15] C. D. Jones,[15] M. Lohner,[15] C. Prescott,[15] J. Yelton,[15] J. Zheng,[15] G. Brandenburg,[16] R. A. Briere,[16] A. Ershov,[16] Y. S. Gao,[16] D. Y.-J. Kim,[16] R. Wilson,[16] H. Yamamoto,[16] T. E. Browder,[17] Y. Li,[17] J. L. Rodriguez,[17] T. Bergfeld,[18] B. I. Eisenstein,[18] J. Ernst,[18] G. E. Gladding,[18] G. D. Gollin,[18] R. M. Hans,[18] E. Johnson,[18] I. Karliner,[18] M. A. Marsh,[18] M. Palmer,[18] M. Selen,[18] J. J. Thaler,[18] K. W. Edwards,[19] A. Bellerive,[20] R. Janicek,[20] D. B. MacFarlane,[20] P. M. Patel,[20] A. J. Sadoff,[21] R. Ammar,[22] P. Baringer,[22] A. Bean,[22] D. Besson,[22] D. Coppage,[22] C. Darling,[22] R. Davis,[22] N. Hancock,[22] S. Kotov,[22] I. Kravchenko,[22] N. Kwak,[22] S. Anderson,[23] Y. Kubota,[23] S. J. Lee,[23] J. J. O'Neill,[23] S. Patton,[23] R. Poling,[23] T. Riehle,[23] V. Savinov,[23] A. Smith,[23] M. S. Alam,[24] S. B. Athar,[24] Z. Ling,[24] A. H. Mahmood,[24] H. Severini,[24] S. Timm,[24] F. Wappler,[24] A. Anastassov,[25] J. E. Duboscq,[25] D. Fujino,[25,§] K. K. Gan,[25] T. Hart,[25] K. Honscheid,[25] H. Kagan,[25] R. Kass,[25] J. Lee,[25] M. B. Spencer,[25] M. Sung,[25] A. Undrus,[25,**] R. Wanke,[25]

[*]Permanent address: Yonsei University, Seoul 120-749, Korea.

[†]Permanent address: Brookhaven National Laboratory, Upton, NY 11973.

[‡]Permanent address: University of Texas, Austin TX 78712

[§]Permanent address: Lawrence Livermore National Laboratory, Livermore, CA 94551.

[**]Permanent address: BINP, RU-630090 Novosibirsk, Russia.

A. Wolf,[25] and M. M. Zoeller[25]

[1]University of Oklahoma, Norman, Oklahoma 73019
[2]Purdue University, West Lafayette, Indiana 47907
[3]University of Rochester, Rochester, New York 14627
[4]Stanford Linear Accelerator Center, Stanford University, Stanford, California 94309
[5]Southern Methodist University, Dallas, Texas 75275
[6]Syracuse University, Syracuse, New York 13244
[7]Vanderbilt University, Nashville, Tennessee 37235
[8]Virginia Polytechnic Institute and State University, Blacksburg, Virginia 24061
[9]Wayne State University, Detroit, Michigan 48202
[10]California Institute of Technology, Pasadena, California 91125
[11]University of California, San Diego, La Jolla, California 92093
[12]University of California, Santa Barbara, California 93106
[13]University of Colorado, Boulder, Colorado 80309-0390
[14]Cornell University, Ithaca, New York 14853
[15]University of Florida, Gainesville, Florida 32611
[16]Harvard University, Cambridge, Massachusetts 02138
[17]University of Hawaii at Manoa, Honolulu, Hawaii 96822
[18]University of Illinois, Champaign-Urbana, Illinois 61801
[19]Carleton University, Ottawa, Ontario, Canada K1S 5B6
and the Institute of Particle Physics, Canada
[20]McGill University, Montréal, Québec, Canada H3A 2T8
and the Institute of Particle Physics, Canada
[21]Ithaca College, Ithaca, New York 14850
[22]University of Kansas, Lawrence, Kansas 66045
[23]University of Minnesota, Minneapolis, Minnesota 55455
[24]State University of New York at Albany, Albany, New York 12222
[25]Ohio State University, Columbus, Ohio 43210

I. INTRODUCTION

Decays of the τ lepton present a unique opportunity to confirm and further probe the Standard Model. The large mass of the τ lepton makes possible decays into hadrons in an environment where the initial state is simple and well understood [2]. This allows comparison with hadron production at comparable center of mass energies from processes such as pion-nucleon, nucleon-nucleon and electron-positron collisions. Strange τ-decays give us information on $SU(3)_f$ symmetry breaking, and direct measurements of the Cabibbo angle (θ_c). The rates for such Cabibbo-suppressed decays ($\tau \to K\nu_\tau, \tau \to K^*\nu_\tau$, and $\tau \to K_1\nu_\tau$, e.g.) can be predicted using corresponding measurements of the Cabibbo favored modes ($\tau \to \pi\nu_\tau$, $\tau \to \rho\nu_\tau$, and $\tau \to a_1\nu_\tau$). For the case of the vector coupling the theoretically expected ratio of branching ratios, $BR(\tau \to K^*\nu_\tau) : BR(\tau \to \rho\nu_\tau)$ [4] can be written, e.g., following the approach of the Das-Mathur-Okubo sum rules [3], as $f(m_{K^*}, m_\rho, m_\tau) \tan^2\theta_c(g^2_{K^*}/g^2_\rho)$ where f is a factor that incorporates the phase space available for decays into ρ and K^*, θ_c is the Cabibbo angle, and the factors g_{K^*} and g_ρ reflect the coupling strengths of the K^* and ρ to the vector current. In the limit of exact SU(3) symmetry, there is no differentiation between the K^{*-} and the ρ^-, so $g_{K^*} = g_\rho$. In the more realistic case of broken symmetry, however, the couplings g are directly proportional to mass. In this approximation, using $\tan^2\theta_c$=0.05, the ratio of rates equals 0.068. There are many experimental results for $\tau \to K^*\nu_\tau$ (where the charged K^* is observed through the very clean decay chain: $K^* \to K^0_S\pi$; $K^0_S \to \pi^+\pi^-$) which are in agreement with this latter prediction [1].

We expect similar relationships to hold for the coupling of the tau to the axial vector K_1 resonance relative to the a_1 resonance. Unfortunately, $\tau \to K_1\nu_\tau$ is not as well-studied as $\tau \to K^{*-}\nu_\tau$, in part due to the fact that $\tau \to K_1$ most often leads to multi-prong events that include charged kaons. Whereas the K^{*-} can be unambiguously identified through its decay, $K^{*-} \to K^0_S\pi^-$, a measurement of charged kaons requires good K/π particle identification in order to separate kaons from the substantially more numerous pions. Moreover, theoretical understanding of charged kaon production in tau decay is hampered by uncertainties in the production mechanism - there is a wide range of predictions for the mass spectrum (expected to be dominated by $K_1(1270)$ and $K_1(1400)$), the $K^*\pi/K\rho$ ratio (in $K\pi\pi$), and helicity amplitudes for τ decays to kaons.

In recent years the large data samples accumulated at CLEO and LEP have allowed much-improved measurements of inclusive decays of tau leptons to charged kaons, complementing similar measurements of inclusive decays of tau leptons to neutral kaons. In this analysis we measure the ratio of branching fractions of $\tau^- \to K^-h^+\pi^-(\pi^0)\nu_\tau$ and $\tau^- \to K^-K^+\pi^-(\pi^0)\nu_\tau$ relative to $\tau^- \to h^-h^+h^-(\pi^0)\nu_\tau$, where $h^\pm$ can be either a charged pion or kaon.

II. DATA SAMPLE AND EVENT SELECTION

Our data sample contains approximately 4.3 million τ-pairs produced in e^+e^- collisions, corresponding to an integrated luminosity of 4.4 fb^{-1}. The data were collected with the CLEO-II detector [5] at the Cornell Electron Storage Ring operating at a center-of-mass energy approximately 10.58 GeV.

The CLEO II detector is a general purpose solenoidal magnet spectrometer and calorimeter. The detector was designed for efficient triggering and reconstruction of two-photon, tau-pair, and hadronic events. Measurements of charged particle momenta are made with three nested coaxial drift chambers consisting of 6, 10, and 51 layers, respectively. These chambers fill the volume from r=3 cm to r=1 m, with r the radial coordinate relative to the beam ($\hat{z}$) axis. This system is very efficient ($\epsilon \geq$98%) for detecting tracks that have transverse momenta (p_T) relative to the beam axis greater than 200 MeV/c, and that are contained within the good fiducial volume of the drift chamber ($|\cos\theta| <$0.94, with θ defined as the polar angle relative to the beam axis). Below this threshold, the charged particle detection efficiency in the fiducial volume decreases to approximately 90% at $p_T \sim$100 MeV/c. For $p_T <$100 MeV/c, the efficiency decreases roughly linearly to zero at a threshold of $p_T \approx$30 MeV/c. This system achieves a momentum resolution of $(\delta p/p)^2 = (0.0015p)^2 + (0.005)^2$ (p is the momentum, measured in GeV/c). Pulse height measurements in the main drift chamber provide specific ionization resolution of 5.5% for Bhabha events, giving good K/π separation for tracks with momenta up to 700 MeV/c and separation of order 2σ in the relativistic rise region above 2 GeV/c. Outside the central tracking chambers are plastic scintillation counters, which are used as a fast element in the trigger system and also provide particle identification information from time-of-flight measurements.

Beyond the time of flight system is the electro-magnetic calorimeter, consisting of 7800 thallium-doped CsI crystals. The central "barrel" region of the calorimeter covers about 75% of the solid angle and has an energy resolution which is empirically found to follow:

$$\frac{\sigma_{\rm E}}{E}(\%) = \frac{0.35}{E^{0.75}} + 1.9 - 0.1E; \tag{1}$$

E is the shower energy in GeV. This parameterization includes effects such as noise, and translates to an energy resolution of about 4% at 100 MeV and 1.2% at 5 GeV. Two end-cap regions of the crystal calorimeter extend solid angle coverage to about 95% of 4π, although energy resolution is not as good as that of the barrel region. The tracking system, time of flight counters, and calorimeter are all contained within a 1.5 Tesla superconducting coil. Flux return and tracking chambers used for muon detection are located immediately outside the coil and in the two end-cap regions.

We select $e^+e^- \to \tau^+\tau^-$ events having a "1vs3" topology in which one τ-lepton decays into one charged particle (plus possible neutrals), and the other τ-lepton decays into 3 charged hadrons (plus possible neutrals). An event is separated into two hemispheres based on the measured event thrust axis[1]. Loose cuts on ionization measured in the drift chamber and energy deposited in the calorimeter are applied on charged tracks in the signal (3-prong) hemisphere to reject leptons. To reduce the background from two-photon collisions ($e^+e^- \to e^+e^-\gamma\gamma$; $\gamma\gamma \to$hadrons and $\gamma\gamma \to l^+l^-$), cuts on visible energy (E_{vis}) and total event transverse momentum (P_t) are applied: $2.5GeV < E_{vis} < 10GeV$, and $P_t > 0.3GeV/c$. We also require the invariant mass of the tracks and showers in the 3-prong hemisphere to be consistent with true τ decays: $M_{3-prong} < 1.7GeV/c^2$.

---

[1]The thrust axis of an event is chosen so that the sum of transverse (to this axis) momenta of all charged tracks has a minimum value.

Events are accepted for which the tag hemisphere (1-prong side) is consistent with one of the following 4 decays: $\tau^- \to e^-\overline{\nu}_e\nu_\tau$, $\tau^- \to \mu^-\overline{\nu}_\mu\overline{\nu}_\tau$, $\tau^- \to \pi^-\nu_\tau$, or $\tau^- \to \rho^-\nu_\tau$. On the 3-prong side of the event, candidate events with and without π^0's are distinguished by the characteristics of showers in the electro-magnetic calorimeter. A 'photon' candidate is defined as a shower in the barrel (end-cap) region of the electro-magnetic calorimeter with energy above $40MeV$ ($60MeV$) and having an energy deposition pattern consistent with true photons. It must be separated from the closest charged track by at least 20 degrees. $Kh\pi$ and $KK\pi$ candidates are defined as those events having zero or one photons in the 3-prong hemisphere. For the $Kh\pi\pi^0$ and $KK\pi\pi^0$ decay modes there must be at least two photons in the signal hemisphere, provided that no more than two photon candidates have a shower energy above 300 MeV. The two most energetic photons in this hemisphere are then paired to form π^0 candidates.

For the $\tau^- \to K^-h^+\pi^-(\pi^0)\nu_\tau$ analysis, we determine the kaon and pion yields, using the 2 same-sign tracks from the three-prong hemisphere. For the $\tau^- \to K^-K^+\pi^-(\pi^0)\nu_\tau$ mode, only the track having sign opposite to its parent τ is considered as a candidate kaon. Note that we implicitly assume that all signal kaons originating from τ decays in our selected 1vs3 samples come from one of the decay modes $\tau^- \to K^-\pi^+\pi^-\nu_\tau$, $\tau^- \to K^-K^+\pi^-\nu_\tau$, $\tau^- \to K^-\pi^+\pi^-\pi^0\nu_\tau$, or $\tau^- \to K^-K^+\pi^-\pi^0\nu_\tau$. The decays $\tau^- \to \pi^-K^+\pi^-\nu_\tau$ and $\tau^- \to K^-\pi^+K^-\nu_\tau$ are prohibited in the Standard Model and have not been experimentally observed, and the decay rate $\tau^- \to K^-K^+K^-\nu_\tau$ is expected be of order 1% relative to that for $\tau^- \to K^-\pi^+\pi^-\nu_\tau$ due to the limited phase space and the low probability of $(s\bar{s})$ pair popping.

III. SIGNAL EXTRACTION PROCEDURE

To find the number of events with kaons, we use specific ionization (dE/dx) information from the central drift chamber. For each track we calculate the deviation of the measured energy loss relative to that expected for true kaons in units of the measured dE/dx resolution ('σ_k'). For true kaons (taken from a data sample of $D^{*+} \to D^0\pi^+; D^0 \to K^-\pi^+$ events), this variable is distributed as a unit Gaussian centered at 0. For pion tracks σ_k also has a Gaussian-like shape but with the mean shifted from zero in a momentum-dependent manner. In this analysis we concentrate on those tracks having momentum $p_{track} > 1.5GeV/c$. Although the K/π separation is better at low momenta than in the relativistic rise regime, we focus on this high momentum region because the separation varies only slowly through this regime and the systematics of signal extraction are therefore somewhat more tractable. Non-τ background as well as the pion background relative to the desired kaon signal in real τ-decays is also smaller at high momenta. These tracks typically have the highest momentum of the tracks in the three-prong hemisphere, and are generally well-separated spatially from the lower momentum tracks.

The number of kaon and pion tracks in the three-prong hemisphere is found statistically by fitting the σ_k distribution for charged tracks to the sum of the pion σ_k shape plus the kaon σ_k shape. Since the kaon-pion separation is modest, it is critical that the shape of the σ_k distribution for pions is well understood. $K_s^0 \to \pi^-\pi^+$ decays provide a very clean sample of true pions from which this distribution can be determined from data. We approximate the pion distribution by a Johnson distribution [6,7] with mean shifted from zero. The

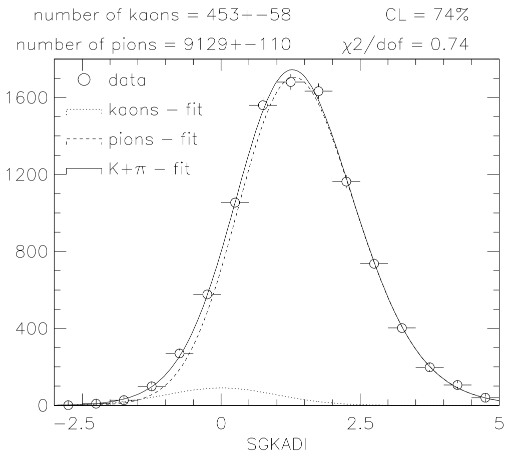

FIG. 1. Fit to σ_k distribution for charged tracks in the 3-prong hemisphere of candidate $\tau\tau$ events, with the fitted kaon and pion curves overlaid.

kaon shape used is a standard unit Gaussian centered at zero[2]. The fitted area under the kaon curve directly yields the number of kaons and the area under the pion curve yields the number of pions.

Requirements on the minimum number of hits used in the dE/dx calculation ($\geq$20, out of 49 possible) and the polar angle of the candidate kaon track ($|\cos\theta| < 0.8$, where θ is the polar angle of the track relative to the positron beam direction) ensure that the track is contained in the good fiducial volume of the drift chamber and that the dE/dx information for the track is of high quality. Since the K/π separation depends on the number of hits ('N_{hit}'), as well as momentum ('p_{track}'), we perform separate σ_k fits for different bins in the two parameter (N_{hit}, p_{track}) space. The kaon and pion yields for each momentum bin above our minimum momentum of 1.5 GeV/c are thereby extracted knowing the pion (and kaon) σ_k shapes for each N_{hit} interval over a specified momentum range. An example of a σ_k fit, showing the kaon and pion components, is displayed in Fig. 1. The $K:\pi$ mixture in this example is typical of the $\tau^- \to K^-h^+\pi^-\nu_\tau$ analysis (of the order $1:20$) and is prepared using all tracks with momentum $1.9GeV/c < P < 2.1GeV/c$.

To determine the total number of $\tau \to KX$ events, we must extrapolate from our measured yields in the region $p_{track} > 1.5$ GeV/c to the lower track momentum region. This is done by fitting the measured kaon and pion spectra to the spectra expected from Monte Carlo simulations in the $p_{track} > 1.5$ GeV/c region, and integrating the fitted Monte Carlo curves over the entire kinematically allowed momentum range. Uncertainties in the appropriate model used to fit the data momentum spectrum are included in our systematic error.

The reconstructed momentum spectrum in the $\tau^- \to K^-h^+\pi^-\nu_\tau$ analysis is shown in Fig. 2, with the Monte Carlo fit overlaid. For decay modes with π^0's, σ_k distributions are made and fitted separately for cases in which the two-photon invariant mass falls in the π^0 region and the π^0 sideband region. Subtracting the K/π yields from the π^0 sidebands, the K/π

---

[2]The difference in kaon yields obtained using a Johnson distribution rather than a unit Gaussian to represent the kaon σ_k distribution is typically less than 1%.

Decay mode	# of K/π reconstructed	hadronic background, %	τ feed-across, %
$Kh\pi\nu/\pi\pi\pi\nu$	$5532 \pm 248/212537 \pm 1002$	1.4/0.09	7.3/9.5
$Kh\pi\pi^0\nu/\pi\pi\pi\pi^0\nu$	$777 \pm 138/55398 \pm 731$	2.1/0.12	9.5/5.7
$KK\pi\nu/\pi\pi\pi\nu$	$1746 \pm 179/107045 \pm 643$	2.1/0.08	4.0/12.6
$KK\pi\pi^0\nu/\pi\pi\pi\pi^0\nu$	$170 \pm 92/26454 \pm 477$	3.8/0.10	0/9.0

TABLE I. Kaon and pion yields in our 1vs3 samples and estimates of background levels. Errors are statistical only. In each pair of numbers in the Table the first number pertains to kaons and the second to pions.

signals associated with true π^0 production can be determined, and the $\tau^- \to K^- h^+ \pi^- \pi^0 \nu_\tau$ yield can be extracted. The number of reconstructed hadrons of both types is presented in Table I.

IV. BACKGROUND

There are two primary sources of background - background from continuum hadronic events ($e^+e^- \to q\bar{q} \to hadrons$) and background from non-signal τ decays (τ 'feed-across'). Hadronic background is estimated using a continuum hadronic Monte Carlo sample (using the JETSET v7.3 [8] event generator) corresponding to the total luminosity of the data sample. The kaon and pion momentum spectra resulting from q$\bar{\text{q}}$ events that satisfy our event cuts are found from this Monte Carlo sample and subtracted from the reconstructed K/π spectra in data prior to fitting for the $\tau \to K^{\pm}$X and $\tau \to \pi^{\pm}$X yields. The level of hadronic background is shown in Table I.

In this analysis, tau decay modes containing K^0_S's are considered feed-across background. Under this definition, the major source of τ background to $\tau \to Kh\pi(\pi^0)\nu$ is found to be $\tau^- \to K^- K^0(\pi^0)\nu_\tau$ decays, in which $K^0_S \to \pi^+\pi^-$. There is also contamination of modes without π^0's from modes with π^0's, and vice versa, which we also determine from Monte Carlo simulations, using our measured branching fractions as inputs. Three prong decays with kaons and more than one π^0 are expected to be severely phase space suppressed and are neglected in this analysis. The approximate level of τ background is given in Table I.

V. NUMERICAL RESULTS

We determine the ratio of branching fractions relative to the normalizing modes directly from the fitted number of kaon and pion tracks in the 1vs3 sample. For the $\tau^- \to K^- h^+ \pi^- \nu_\tau$ and $\tau^- \to K^- h^+ \pi^- \pi^0 \nu_\tau$ decay modes, each event contributes 2 same-sign tracks to the analyzed sample of tracks, one of which is a kaon and one a pion. By contrast, $\tau^- \to \pi^-\pi^+\pi^-\nu_\tau$ events contribute 2 pions. Straightforward algebra can be used to find a simple expression for the desired ratio of branching fractions, as outlined in the Appendix. This calculation gives us the results for the ratios ($'R'$) of branching fractions shown in Table II. The first error shown is statistical and the second is systematic. For each ratio, we multiply

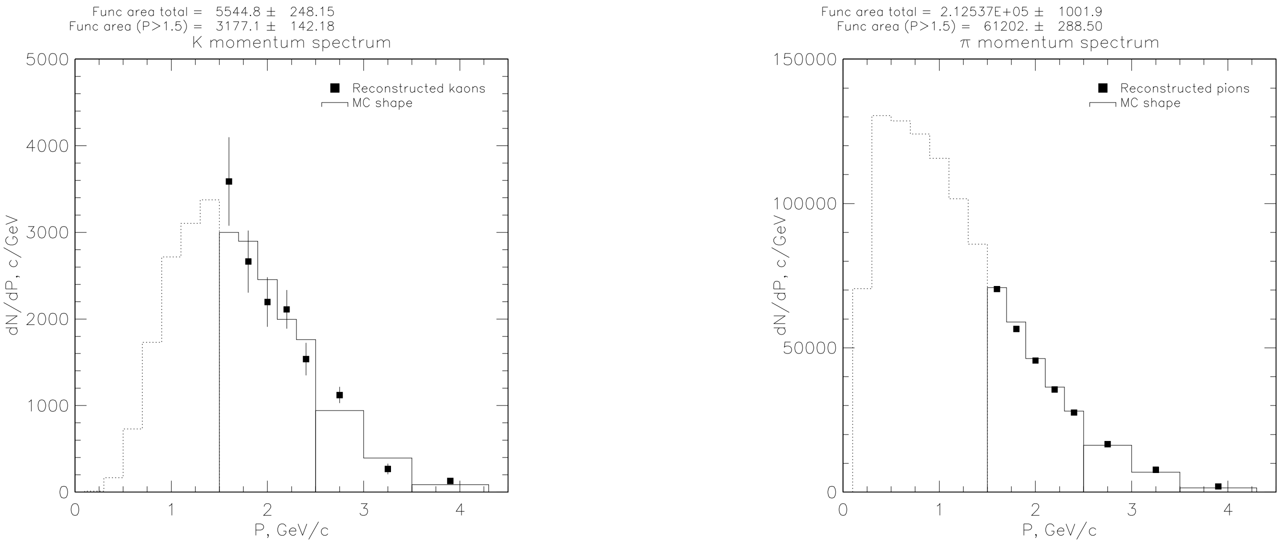

FIG. 2. Reconstructed kaon (left) and pion (right) momentum spectra for $\tau \to Kh\pi\nu_\tau$ candidates.

Decay Mode	Ratio 'R' ($\times 10^{-2}$)	Absolute BR, %
$\tau \to Kh\pi\nu_\tau$	$\frac{Br(\tau\to Kh\pi\nu_\tau)}{Br(\tau\to\pi\pi\pi\nu_\tau)}$=$5.24 \pm 0.24 \pm 0.73$	$0.488 \pm 0.023 \pm 0.068$
$\tau \to Kh\pi\pi^0\nu_\tau$	$\frac{Br(\tau\to Kh\pi\pi^0\nu_\tau)}{Br(\tau\to Kh\pi\pi^0\nu_\tau)}$=$2.71 \pm 0.48 \pm 0.49$	$0.117 \pm 0.021 \pm 0.021$
$\tau \to KK\pi\nu_\tau$	$\frac{Br(\tau\to KK\pi\nu_\tau)}{Br(\tau\to\pi\pi\pi\nu_\tau)}$=$1.72 \pm 0.18 \pm 0.29$	$0.160 \pm 0.017 \pm 0.026$
$\tau \to KK\pi\pi^0\nu_\tau$	$\frac{Br(\tau\to KK\pi\pi^0\nu_\tau)}{Br(\tau\to\pi\pi\pi\pi^0\nu_\tau)}$=$0.77 \pm 0.42 \pm 0.15$	$0.033 \pm 0.018 \pm 0.007$

TABLE II. Results

by the currently tabulated branching fractions [1] for the normalizing modes to determine an absolute branching fraction for each $\tau \to KX$ mode, as indicated in Table II.

VI. SYSTEMATIC ERRORS

The breakdown of systematic errors in our calculation of the ratio of branching fractions for each decay mode is given in Table III. Our dominant systematic errors arise from our uncertainty in the fit procedure used to determine the number of kaons and pions in the 1vs3 sample and from the choice of decay models in MC. The former error was estimated by performing cross-checks on independent mixtures of kaons and pions with known fractions of particles of each type. Tagged samples of kaons and pions were obtained using data events in which $D^{*+} \to D^0\pi^+$, and the D^0 decays to either $K^-\pi^+$ or $K^-\pi^+\pi^-\pi^+$, or $\phi \to K^+K^-$. The σ_k distributions of kaons and pions were subsequently added in proportions roughly equivalent to those found in our signal three-prong tau decays and the signal extraction procedure applied. The number of fitted kaons was then compared to the true number of input kaons, and a ratio $(\frac{N_{fit}}{N_{true}})$ was determined. The results are shown in Table IV. The results of these cross-checks were used to estimate the systematic errors inherent in the signal

Source	$\frac{Kh\pi\nu}{\pi\pi\pi\nu}$	$\frac{Kh\pi\pi^0\nu}{\pi\pi\pi^0\nu}$	$\frac{KK\pi\nu}{\pi\pi\pi\nu}$	$\frac{KK\pi\pi^0\nu}{\pi\pi\pi^0\nu}$
Kaon extraction procedure	10%	11%	12%	14%
MC Model uncertainties	7%	8%	10%	10%
τ MC branching fraction uncertainties	2%	8%	2%	1%
MC statistics (for efficiencies)	1%	3%	2%	6%
$q\bar{q}$ background	1%	2%	2%	4%
Other backgrounds (2γ, QED, beam-gas)	5%	5%	5%	5%
Photon finding/veto	4%	4%	4%	4%
Tracking, Trigger, Tag ID	cancels	cancels	cancels	cancels
Total	14%	18%	17%	20%

TABLE III. Systematic errors

Cross-check	Mixture type	$\frac{N_{fit}}{N_{true}}$	Systematic error
$D^0 \to K^-\pi^+$	as in $Kh\pi$	0.934 ± 0.071	10.2%
	as in $Kh\pi\pi^0$	0.925 ± 0.079	11.4%
	as in $KK\pi$	0.931 ± 0.093	11.6%
	as in $KK\pi\pi^0$	0.904 ± 0.094	14.3%
$\phi \to K^+K^-$	$K : \pi \approx 1:1 - 1:3$	1.014 ± 0.021	-
$D^0 \to K^-\pi^+\pi^-\pi^+$	$K : \pi \approx 1:10$	0.999 ± 0.251	-

TABLE IV. Summary of cross-checks and systematic errors of signal extraction.

extraction procedure. Note that we use the same sample of kaons and pions (varying the relative amounts) to derive all of the ratios presented in Table IV; there is thus a strong correlation between all of the indicated ($\frac{N_{fit}}{N_{true}}$) ratios. We therefore do not make an explicit numerical correction to our final results based on these numbers, but instead only use the amount by which they differ from unity to assess our systematic errors.

The MC modeling error listed in Table III includes our uncertainty in fitting the extracted pion and kaon momentum spectra (i.e., extrapolating into the p_{track} <1.5 GeV/c region), as well as the efficiencies for Monte Carlo events to pass our event and track selection criteria. To evaluate this error, a variety of decay models, both resonant and non-resonant, were used to determine the possible shapes of the $\frac{dN}{dp_{track}}$ spectra and recalculate branching ratios.[3] Since τ decay modes with kaons are not well understood theoretically, and since data on such decays is sparse, this uncertainty is somewhat large (see Table III).

To estimate the systematic error in our feed-across estimate due to the uncertainty in the input tau decay branching fractions, several different samples of generic τ Monte Carlo

[3] The following models were investigated: for $\tau \to K^-\pi^+\pi^-\nu_\tau$: $\tau \to K_1(1270)\nu_\tau$, $\tau \to K_1(1430)\nu_\tau$, phase space; for $\tau \to K^-K^+\pi^-\nu_\tau$: $\tau \to K^{*0}K^-\nu_\tau$, $\tau \to \rho(1690)^-\nu_\tau$ ($\rho(1690)^- \to K^{*0}K^-$), phase space; for $\tau \to K^-\pi^+\pi^+\pi^0\nu_\tau$: $\tau \to K^-\omega\nu_\tau$ and phase space; for $\tau \to K^-K^+\pi^-\pi^0\nu_\tau$: $\tau \to \rho(1690)^-\nu_\tau$ ($\rho(1690)^- \to K^{*-}K^*0$), phase space.

were generated using the KORALB package, with branching fractions of the components changed within $\pm 1\sigma$ of the 'best' known value. Most feed-across corrections are determined using branching fractions from the Particle Data Group [1]; the magnitude of feed-across corrections internal to this measurement (e.g., $\tau \to K^-\pi^+\pi^-\pi^0\nu_\tau$ contamination of $\tau \to K^-\pi^+\pi^-\nu_\tau$) are taken from the results of this analysis. The quoted systematic error is derived from the observed variation of the final results when the input branching fractions are varied.

We conservatively assign a 100% systematic error on the hadronic background level (see Table II), given the possibility that our hadronic simulation may not accurately model the $q\bar{q}$ background. Remaining backgrounds, namely 2-photon events, beam-gas interactions, and QED background are assessed by varying our event and track selection requirements and determined to be less than 5%. To take into account systematics related to photon-finding, as well as our neutral energy veto, we assign a 4% systematic error for each mode (Table III).

Our Monte Carlo samples have limited statistics so we assign an error corresponding to the statistical error on the efficiencies and feed-across corrections determined from Monte Carlo simulations. There are other systematic effects that cancel in the final ratio of branching fractions such as trigger efficiencies, tag identification requirements and track-finding systematics.

VII. SUMMARY

We have measured the ratios of branching fractions:

- $Br(\tau^- \to K^-h^+\pi^-\nu_\tau)/Br(\tau^- \to \pi^-\pi^+\pi^-\nu_\tau) = (5.24 \pm 0.24 \pm 0.73) \times 10^{-2}$,
- $Br(\tau^- \to K^-h^+\pi^-\pi^0\nu_\tau)/Br(\tau^- \to \pi^-\pi^+\pi^-\pi^0\nu_\tau) = (2.71 \pm 0.48 \pm 0.49) \times 10^{-2}$,
- $Br(\tau^- \to K^-K^+\pi^-\nu_\tau)/Br(\tau^- \to \pi^-\pi^+\pi^-\nu_\tau) = (1.72 \pm 0.18 \pm 0.29) \times 10^{-2}$, and
- $Br(\tau^- \to K^-K^+\pi^-\pi^0\nu_\tau)/Br(\tau^- \to \pi^-\pi^+\pi^-\pi^0\nu_\tau) < 0.0152$ at 95% CL, based on: $Br(\tau^- \to K^-K^+\pi^-\pi^0\nu_\tau)/Br(\tau^- \to \pi^-\pi^+\pi^-\pi^0\nu_\tau) = (0.77 \pm 0.42 \pm 0.15) \times 10^{-2}$.

where contributions to both denominator and numerator from $\tau \to K^0_S X$; $K^0_S(\to \pi^+\pi^-)$ have been excluded. If we instead normalize to $\tau \to h^-h^+h^-(\pi^0)\nu_\tau$, the corresponding ratio of branching fractions are:

- $Br(\tau^- \to K^-h^+\pi^-\nu_\tau)/Br(\tau^- \to h^-h^+h^-\nu_\tau) = (4.98 \pm 0.23 \pm 0.69) \times 10^{-2}$,
- $Br(\tau^- \to K^-h^+\pi^-\pi^0\nu_\tau)/Br(\tau^- \to h^-h^+h^-\pi^0\nu_\tau) = (2.64 \pm 0.47 \pm 0.48) \times 10^{-2}$,
- $Br(\tau^- \to K^-K^+\pi^-\nu_\tau)/Br(\tau^- \to h^-h^+h^-\nu_\tau) = (1.63 \pm 0.17 \pm 0.27) \times 10^{-2}$, and
- $Br(\tau^- \to K^-K^+\pi^-\pi^0\nu_\tau)/Br(\tau^- \to h^-h^+h^-\pi^0\nu_\tau) < 0.0148$.

Subtracting decay modes with two charged kaons from the results above we can calculate the ratios of branching fractions: $Br(\tau^- \to K^-\pi^+\pi^-\nu_\tau)/Br(\tau^- \to h^-h^+h^-\nu_\tau) = (3.35 \pm 0.29 \pm 0.74) \times 10^{-2}$, and $Br(\tau^- \to K^-\pi^+\pi^-\pi^0\nu_\tau)/Br(\tau^- \to h^-h^+h^-\pi^0\nu_\tau) = (1.89 \pm 0.62 \pm 0.50) \times 10^{-2}$.

τ decay mode	Measurement	Branching fraction, 10^-2
$\tau^- \to K^0\pi^-\pi^0\nu_\tau$	ALEPH [12]	$0.32 \pm 0.11 \pm 0.05$
	CLEO [14]	$0.417 \pm 0.058 \pm 0.044$
$\tau^- \to K^-\pi^+\pi^-\nu_\tau$	ALEPH [16]	$0.214 \pm 0.037 \pm 0.029$
	This analysis	$0.328 \pm 0.028 \pm 0.073$
$\tau^- \to K^-\pi^0\pi^0\nu_\tau$	ALEPH [12]	$0.08 \pm 0.02 \pm 0.02$
	CLEO [15]	$0.14 \pm 0.10 \pm 0.03$
$\tau^- \to K^-K^0\pi^0\nu_\tau$	ALEPH [12]	$0.10 \pm 0.05 \pm 0.03)$
	CLEO [14]	$0.145 \pm 0.036 \pm 0.020$
$\tau^- \to K^-K^+\pi^-\nu_\tau$	ALEPH [16]	$0.163 \pm 0.021 \pm 0.017$
	This analysis	$0.160 \pm 0.017 \pm 0.026$
$\tau \to K_s^0K_L^0\pi^-\nu_\tau$	ALEPH [13]	$0.13 \pm 0.04 \pm 0.02$
$\tau \to K_s^0K_s^0\pi^-\nu_\tau$	CLEO [14]	$0.023 \pm 0.005 \pm 0.003$
$\tau \to K^0\bar{K}^0\pi^-\nu_\tau$	L3 [23]	$0.31 \pm 0.12 \pm 0.04$

TABLE V. Current measurements of $\tau \to Kh\pi\nu_\tau$ decay modes.

VIII. DISCUSSION

The $\tau^- \to K^-\pi^+\pi^-\nu_\tau$ decay mode is believed to occur predominantly through coupling to the axial-vector mesons $K_1(1270)$ and $K_1(1400)$. It is known that the $K_1(1270)$ decays mostly into $K\rho$ while the $K_1(1400)$ decays exclusively into $K^*(892)\pi$ [9,10]. Thus, determining whether the decay chain in such decays is $\tau \to K_1\nu \to K^*\pi\nu \to K\pi\pi\nu$ or $\tau \to K_1\nu \to K\rho\nu \to K\pi\pi\nu$ can allow us to draw conclusions on which resonance dominates in 3-meson τ decays with strangeness. Since we extract the number of kaons relative to the number of pions statistically, in this analysis we do not reconstruct K^* or ρ and therefore can not determine this directly. However we can exploit isospin symmetry relations and compare several experimental results for τ decay into the $K\pi\pi$ final state. Isospin symmetry predicts that the ratio of branching fractions for τ decays into $\bar{K}^0\pi^-\pi^0$, $K^-\pi^+\pi^-$ and $K^-\pi^0\pi^0$ would be 4:4:1 if the decay proceeded through an intermediate $K^*\pi$ or 2:2:0 if the decay proceeded through an intermediate $K\rho$ [11]. At present, there are measurements of these three decay modes by ALEPH abd CLEO, as summarized in Table V. Taken together, these results favor production through the $K^*\pi$ state rather than through $K\rho$, although the experimental errors are still rather large.

Theoretical predictions for the $\tau^- \to K^-\pi^+\pi^-\nu_\tau$ decay mode exist [11] and assume that both the $K_1(1270)$ and $K_1(1400)$ resonances are possible intermediate states for this process. The numerical prediction for this branching fraction calculated by Finkemeier and Mirkes [11] is 0.77%, approximately twice as large as our current analysis, as well as other measurements (ALEPH, for example, obtained $(0.228 \pm 0.039 \pm 0.027) \times 10^{-2}$ [16]). Another theoretical prediction, 0.18% by Li [22], is more consistent with experiment. One possible cause for the disagreement between the Finkemeier and Mirkes prediction and experiment [17] may be that incorrect parameters (particularly the full width of the K_1 resonances appropriate for tau decays) were used in that theoretical calculation [17].

In contrast to the $K\pi\pi$ mode, tau decays into the 3-meson final state with two kaons ($\tau^- \to K^- K^+ \pi^- \nu_\tau$) may occur through either the vector or axial vector currents. Theoretical predictions for the fraction of $V : A$ vary considerably ([19–22]). Recent work [11,21] suggests that the axial-vector contribution in this decay is larger. These latter models include both the $K^* K$ and $\rho\pi$ intermediate states. As in the case of the $K\pi\pi$ decay mode, one can use isospin symmetry to relate $K^- K^0 \pi^0$, $K^- K^+ \pi^-$ and $K^0 \bar{K}^0 \pi^-$ tau decays. The ratio of the branching fractions of these decay modes should be 2:1:1 if $\tau^- \to K^- K^+ \pi^- \nu_\tau$ proceeds exclusively through the $\rho\pi$ intermediate state or 1:1:1 if this decay proceeds through $K^* K$. The experimental results for these decay modes are given in Table V. The decay rate of $\tau \to K^0 \bar{K}^0 \pi^- \nu_\tau$ can be inferred from the ALEPH's measurement of $Br(\tau \to K^0_S K^0_L \pi^- \nu_\tau)$ and the CLEO measurement $Br(\tau \to K^0_S K^0_S \pi^- \nu_\tau)$ (Table V). These results imply $(0.26 \pm 0.08 \pm 0.04) \times 10^{-2}$ and $(0.092 \pm 0.020 \pm 0.012) \times 10^{-2}$ for $\tau \to K^0 \bar{K}^0 \pi^- \nu_\tau$, provided that the $K^0 \bar{K}^0$ system evolves incoherently. Comparison of these numbers with the isospin-predicted ratios indicates that the bulk of $KK\pi$ production occurs through the $K^* K$ intermediate state. This conclusion is consistent with the direct measurement of $\frac{\mathcal{B}(\tau \to K^* K \nu_\tau)}{\mathcal{B}(\tau \to K^- K^+ \pi^- \nu_\tau)}$=0.87±0.13 by ALEPH [16].

The theoretical prediction for the $\tau^- \to K^- K^+ \pi^- \nu_\tau$ decay mode is $\sim 0.2\%$ in [11]. Our measurement $(0.160 \pm 0.017 \pm 0.026) \times 10^{-2}$ is close to this value and is also consistent with the latest ALEPH measurement of this mode $(0.168 \pm 0.022 \pm 0.020) \times 10^{-2}$ [16].

The theory of τ decay into 4-meson final states with kaons ($\tau^- \to K^- \pi^+ \pi^- \pi^0 \nu_\tau$ and $\tau^- \to K^- K^+ \pi^- \pi^0 \nu_\tau$, e.g.) is more difficult to formulate than that for the 3-meson decays discussed above due to the substantially larger number of possible intermediate states. Li [22] has calculated $\tau \to \omega K \nu_\tau$=0.025%, which, if correct, would account for approximately 1/4 of our observed total $\tau^- \to K^- \pi^+ \pi^- \pi^0 \nu_\tau$. Unfortunately, we do not yet have the requisite sensitivity to verify this prediction. Explicit measurements of the substructure in $\tau \to \pi^- \pi^+ \pi^- \pi^0 \nu_\tau$, coupled with these results (Table II) and ALEPH ($Br(\tau^- \to K^- \pi^+ \pi^- \pi^0 \nu_\tau) = (0.061 \pm 0.039 \pm 0.018) \times 10^{-2}$ and $Br(\tau^- \to K^- K^+ \pi^- \pi^0 \nu_\tau) = (0.075 \pm 0.029 \pm 0.015) \times 10^{-2}$) may provide guidance for future progress in this sector.

REFERENCES

[1] R. M. Barnett et al., Phys. Rev. **D54**, 1 (1996).

[2] Y. S. Tsai, Phys. Rev. **D4**, 2821 (1971).

[3] T. Das, V. Mathur, and S. Okubo, Phys. Rev. Lett. 18 761 (1967).

[4] S. Oneda, Phys. Rev. **D35**, 397 (1987).

[5] CLEO Collab., Y. Kubota et al., Nucl. Inst. Meth. **320** 66, (1992).

[6] "Systems of frequency curves" by W. P. Elderton and N. L. Johnson, publ. Wiley & Sons, New York, NY, 1994.

[7] "Statistical Models in Engineering" by G. J. Hahn and S. S. Shapiro, publ. Cambridge Univ. Press, London, UK, 1994.

[8] JETSET 7.3: T. Sjöstrand and M. Bengtsson, Comput. Phys. Commun. **43**, 367 (1987).

[9] G. W. Brandenburg et al., Phys Rev. Lett. **36**, 703 (1976).

[10] R. K. Carnegie et al., Nucl. Phys. **B127**, 509 (1977).

[11] M. Finkemeier and E. Mirkes, Z. Phys. **C69**, 243 (1996).

[12] ALEPH Collaboration, D. Buskulic et al., CERN-PPE/95-140 (1995)

[13] ALEPH Collaboratio, EPS95 Ref. EPS0448, contribution to the International Europhysics Conference on High Energy Physics, Brussels, 1995 (unpublished).

[14] CLEO collaboration, T. Coan et al., Phys. Rev. **D53**, 6037 (1996)

[15] CLEO Collaboration, M. Battle et al., Phys. Rev. Lett. **73**, 1079 (1994)

[16] ALEPH Collaboration, R. Barate et al., CERN-PPE/97-69, (1997).

[17] E. Mirkes, Nuclear Physics B (Proc. Suppl.) **55C**, 169, 1997; (Proceedings of *TAU96: Fourth Workshop on Tau Lepton Physics*, Estes Park, Colorado, September 16-19, 1996, ed. J.G. Smith and W. Toki.)

[18] ACCMOR Collaboration, C. Daum et al., Nucl. Phys. **B187**, 1 (1981).

[19] J. J. Gomez-Cadenas, M. C. Gonzalez-Garcia, and A. Pich, Phys. Rev. **D42**, 3093 (1990).

[20] E. Braaten, R. J. Oakes, S. Tse, Int. J. Mod. Phys. **A5**, 2737 (1990)

[21] R. Decker, E. Mirkes, R. Sauer, and Z. Was, Z. Phys. **C58**, 445 (1993).

[22] B. A. Li, Phys. Rev. **D55**, 1436, (1997).

[23] L3 Collaboration, M. Acciarri et al., Phys. Lett. **B352**, 487 (1995).

[24] H. Lipkin, Phys. Let. B 303 (1993) 119.

[25] M. Suzuki, Phys. Rev. **D47**, 1252 (1993).

[26] F. J. Gilman and S. H. Rhie, Phys. Rev. **D31**, 1066 (1985).

IX. APPENDIX: DERIVATION OF RELATIVE RATIO OF BRANCHING FRACTIONS

The expression for the ratio of branching fractions for $Br(\tau \to Kh\pi(\pi^0)\nu_\tau)/Br(\tau \to \pi\pi\pi(\pi^0)\nu_\tau)$ $\tau \to Kh\pi(\pi^0)\nu_\tau)$ is straightforward to derive. Each $\tau \to Kh\pi(\pi^0)\nu_\tau)$ event contributes one kaon and one pion into the analyzed sample of tracks and each $\tau \to \pi\pi\pi(\pi^0)\nu_\tau)$ contributes 2 pions. A system of linear equations can be written from which follows the formula:

$$\frac{Br(\tau \to Kh\pi(\pi^0)\nu_\tau)}{Br(\tau \to \pi\pi\pi(\pi^0)\nu_\tau)} = \frac{N_{Kh\pi(\pi^0)}}{N_{\pi\pi\pi(\pi^0)}} = \frac{N_K^{fit}\phi_{Kh\pi}}{\epsilon_K\phi_{\pi\pi\pi}N_\pi^{fit} - \epsilon_{\pi fk}\phi_{Kh\pi}N_K^{fit}}\frac{2\epsilon_\pi\epsilon_{\pi\pi\pi}}{\epsilon_{Kh\pi}}$$

where N_K^{fit} and N_π^{fit} are the fitted numbers of kaons and pions for a given 1vs3 sample, ϵ_K, $\epsilon_{\pi fk}$ and ϵ_π are the efficiencies for a hadron (kaon or pion from $Kh\pi(\pi^0)$ decay or pion from $\pi\pi\pi(\pi^0)$ decay) to pass our track selection requirements, $\epsilon_{Kh\pi}$ and $\epsilon_{\pi\pi\pi}$ are the efficiencies for the indicated events to pass our 1vs3 event selection cuts, and $\phi_{Kh\pi}$ and $\phi_{\pi\pi\pi}$ represent the τ feed-across corrections.

The expression for the decay modes $\tau^- \to K^-K^+\pi^-\nu_\tau$ and $\tau^- \to K^-K^+\pi^-\pi^0\nu_\tau$ is simpler since only one track is taken from each event:

$$\frac{Br(\tau \to KK\pi(\pi^0)\nu_\tau)}{Br(\tau \to \pi\pi\pi(\pi^0)\nu_\tau)} = \frac{N_{Kh\pi(\pi^0)}}{N_{\pi\pi\pi(\pi^0)}} = \frac{N_K^{obser}\cdot\phi_{Kh\pi}\epsilon_\pi\epsilon_{\pi\pi\pi}}{N_\pi^{obser}\cdot\phi_{\pi\pi\pi}\epsilon_K\epsilon_{Kh\pi}}$$

where the efficiencies and feed-across corrections have the same meaning as in the previous formula. The values of track efficiencies ϵ_K, $\epsilon_{\pi fk}$ and ϵ_π are of the order of 90% for our cuts and the event efficiencies $\epsilon_{Kh\pi}$, $\epsilon_{\pi\pi\pi}$ are of the order of 28% for decays without π^0's and 14% for decays with π^0.